AIChE WILEY InterScience DISCOVER SOMETHING GREAT

Hydrolysis of Olive Oil Using Lipase Bonded to Modified Carbon Membrane

S. Sachan, S. Sachdeva, G. Pugazhenthi, and Anil Kumar
Dept. of Chemical Engineering, Indian Institute of Technology Kanpur, Kanpur 208016, India

DOI 10.1002/aic.10733
Published online December 12, 2005 in Wiley InterScience (www.interscience.wiley.com).

A noninterpenetrating supported carbon membrane was prepared using a resole-type phenol-formaldehyde resin as precursor. Amine groups were created on the carbon membrane through nitration using NO_x and used to immobilize lipase enzyme by reacting with glutaraldehyde. To maintain high enzyme activity, surface carboxylic groups were modified and the immobilized enzyme on the membrane thus obtained was active even after 3 months of usage. The performance of the biphasic membrane reactor is studied in terms of amount of free fatty acid produced per unit time based on the volume of aqueous phase and the effect of operating variables (pH of aqueous phase solution, solvent used for olive oil, olive oil concentration, and aqueous phase circulation rate) were evaluated. Experiments show that the activity of lipase increases 1.42-fold upon immobilization. The maximum reaction rate was 3.6-fold higher, and the base case rate was 1.4-fold higher than the values reported in the literature for a similar enzyme membrane reactor but with a different membrane. © 2005 American Institute of Chemical Engineers *AIChE J,* 52: 1611–1620, 2006

Keywords: carbon-composite membrane, hydrolysis of olive oil, space charge model

Introduction

Enzyme membrane reactors (EMRs) are used for conversion of fats and oils into acids using an ultrafiltration membrane having an immobilized enzyme. The reactor has the advantages of integrating catalytic conversion and product separation into a single operation.[1] There are several immobilization techniques that have been reviewed recently,[2-4] in which it was indicated that a large number of factors influence the performance of the immobilized enzyme. Among these, the selection of support materials and the method of immobilization were found to be most the most critical factors. Various membrane materials (hydrophobic and hydrophilic) and membrane reactor configurations with the enzyme immobilized on internal or external membrane surfaces have been reported in the literature.[2] Hydrophobic membrane reactors have supports prepared from polypropylene,[5] polyvinyl chloride,[6] polyvinyledenedifluoride,[7] or polyetherimide.[8] In these, lipase has been immobilized on the aqueous side of the membrane. In hydrophilic membrane reactors, the lipase has been immobilized on the organic side of the membrane, which was made of cellulose,[9] polyamide,[10] or polyacrylonitrile.[11] Advantages of the hydrophilic system are that the enzyme desorption is reduced because of its insolubility in the organic phase and catalytic activity of the enzyme is found to be much higher than that for the hydrophobic membrane.[12]

In an effort to assess the effect of supports on the performance of EMRs, in our earlier studies we bonded lipase enzyme on zeolite[13] and poly(methyl methacrylate) (PMMA)[14] composite membranes. In this study, we prepared ultrafiltration carbon membranes as follows.[15] The process consisted of carbonizing a film of crosslinked resole-type phenol-formaldehyde (PF) resin film in the absence of air at 500°C. Herein, we have devised a nitration technique using NO_x, which was subsequently reduced to amine groups using its reaction with hydrazine hydrate. The aminated membrane thus formed was reacted with glutaraldehyde to bond the lipase enzyme chemically to it. We have shown that the enzyme membrane thus

Correspondence concerning this article should be addressed to A. Kumar at anilk@iitk.ac.in.

formed is highly acidic and the enzyme tends to be deactivated within two cycles of usage. However, on reacting it to 1,4-phenylenediamine immediately after the nitration step, and then immobilizing the enzyme after amination, the enzyme retains its activity for a considerably long time (at least over 3 months) of usage. The performance of the biphasic EMR is evaluated in terms of the amount of free fatty acid produced per unit time based on the volume of aqueous phase. The effects of different organic solvents (pentane, hexane, and heptane) for the olive oil, the concentration of olive oil, circulation rate of aqueous phase, and the pH of aqueous phase on the performance of the membrane reactor are determined. Based on this kinetic mechanism for hydrolysis of triglycerides given in the literature[16-22] and the mathematical procedure,[13] we showed the membrane capillaries to be charged having a wall potential of 0.71 mV.

Modeling of Biphasic Enzyme Membrane Reactor

The biphasic EMR represents a continuous microenvironment for the reaction; the two reactants, olive oil and water, come in contact with the enzyme at the membrane surface where the reaction and simultaneous separation take place. For continuous extraction of the fatty acid into the aqueous phase the aqueous phase is maintained at a basic pH (8–9.5), by adding an adequate amount of NaOH solution. The pK_a value is about 5 for fatty acids, which are assumed to be completely ionized. Furthermore, the highly nucleophilic OH^- ion combines irreversibly with the carbonyl group (COOH) of fatty acid to form the resonance-stabilized COO^- ions.[23-27] Because the applied pressure is very small, only diffusion resistance to the mass transfer exists.

In a continuous microenvironment, the water molecules are reported to form a monolayer near the active site of the enzyme[28] and, if a reservoir of water is present very near to the active site, then the water concentration can be approximated as constant, as has been done by Molinari et al.[26] The stoichiometric relation can be written as

$$\mathrm{RCOOH} + \mathrm{OH^-} \rightleftharpoons \mathrm{RCOO^-} + \mathrm{H_2O} \qquad (1)$$

The reaction mechanism and thus the rate expression for the hydrolysis are quite complex and the reaction kinetics has been modeled in the literature[29,30] using the Michaelis–Menten model.

Hydrolysis of olive oil occurs at the enzyme located at the pore mouth of the membrane and it generates fatty acid. The fatty acid formed is extracted into the aqueous phase at alkaline pH and, to keep the analysis simple, it is assumed that the fatty acid formed is the oleic acid alone (as done in the reaction kinetic analysis). The extraction is facilitated by reaction of the acid molecule with the OH^- ions, assumed to be instantaneous. Figure 1 shows the mass-transfer phenomenon. In this figure, AA′ represents the reaction front and the oleic acid molecule formed at the enzyme sites (at the pore mouth) migrates toward the reaction front. The OH^- ions in the aqueous phase at the righthand side of AA′ move toward the reaction front where they are consumed and $RCOO^-$ ions are generated. The $RCOO^-$ ions diffuse toward the bulk of the aqueous phase as a result of the concentration gradient. To maintain a constant pH of the aqueous phase, NaOH is continuously added to it,

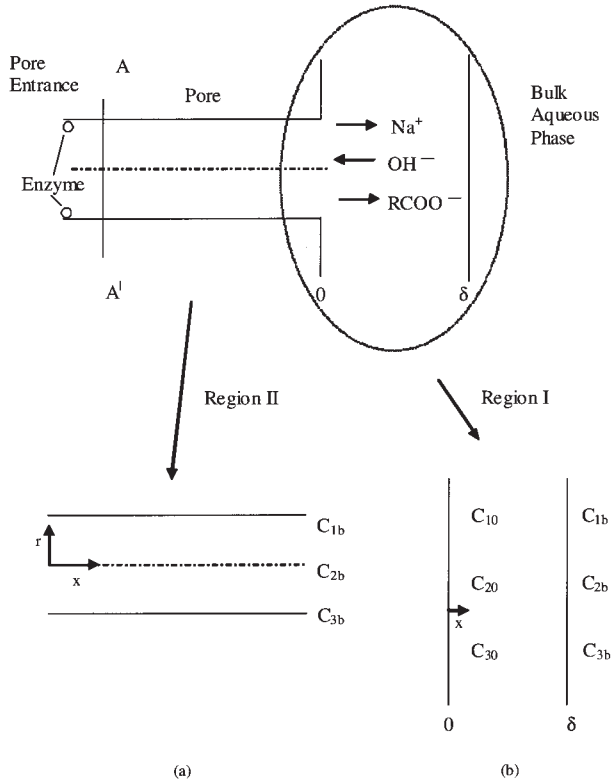

Figure 1. The mass-transfer phenomenon inside the membrane and on the aqueous side of the membrane.

which leads to a buildup of Na^+ ions in the bulk, and these ions diffuse toward the reaction front. The region to the right of the reaction front thus contains Na^+ (hereafter referred to as ion 1), OH^- (hereafter referred to as ion 2), and $RCOO^-$ (hereafter referred to as ion 3) ions and the system involves ternary diffusion of the ions. Because the diffusivity of OH^- ions (5.29×10^{-9} m^2/s) is much greater (~1000-fold) than that of the RCOOH (1.2×10^{-12} m^2/s, evaluated using the modified Wilke–Chang equation[31]), the reaction front is assumed to lie at the pore mouth for the short reaction time considered in this work.

The mass transport phenomenon inside the support of the membrane is assumed to be similar to that outside it and so the entire system can be divided into two regions. The first region consists of an unstirred film from the pore end to the bulk of the aqueous phase. Figure 1b shows region I, consisting of an unstirred film of thickness δ. For a very small rate of mass transfer, the film thickness is related to the mass-transfer coefficient as

$$k = \frac{D}{\delta} \qquad (2)$$

and the mass-transfer coefficient can be evaluated using the following relation for transport through membranes[32].

$$\mathrm{Sh} = \frac{kd}{D} = 0.023\,\mathrm{Re}^{7/8}\mathrm{Sc}^{1/4} \qquad (3)$$

$$\mathrm{Re} = \frac{\rho u d}{\mu} \qquad \text{and} \qquad \mathrm{Sc} = \frac{\mu}{\rho D} \tag{4}$$

where d is the diameter of the cylindrical compartment, ρ is fluid density, μ is fluid viscosity, and u is the velocity of water in the aqueous compartment. The maximum thickness of the film is obtained from this relation and it will be seen later that the actual thickness is much smaller than that calculated from the above expression.

Region II consists of the pore and the ion transport inside the pores is considered to be at steady state and is assumed to be described by space charge model and the fluid velocity inside the pore is zero. The transport of ions is described by the Nernst–Planck equation as (cylindrical coordinates). The nonlinear differential equation, solved analytically in the form of an infinite power series, is given in our earlier publication.[13]

Experimental

Materials

Glutaraldehyde (25%), thionyl chloride, 1,4-phenylenediamine, sodium dihydrogen phosphate, gum arabic, sodium chloride, calcium chloride, sodium tauroglucate salt, sodium hydroxide, olive oil, enzyme (pancreatic lipase), and solvents (toluene, pentane, hexane, and heptane) were procured from SD Fine Chemicals (Mumbai, India).

Preparation of carbon–clay composite membrane

To prepare a porous carbon membrane, the resole-type phenolic resin was prepared by condensation polymerization of phenol (94 g, 1 mol) and 37% aqueous formaldehyde (123 g, 1.5 mol) in the presence of a basic catalyst (5 g, 0.125 mol). For membrane casting, the clay support is dipped in xylene to displace air present inside its pores after which it was placed over a sponge soaked in xylene, thus ensuring that the polymer does not enter into the pores of the support. A solution of resole in ethyl alcohol is spread over the clay support. The coated support is then allowed to dry in air for 1 h followed by curing for 2 h at 60°C and for 12 h at 120°C in an oven. The clay–resole composite is heated at the rate of 2.5–30°C/min up to 500°C and was subsequently carbonized in the absence of air at 500°C for 0.5 h. It is suggested[33] that the carbon film thus formed is acidic and can be represented by the following

in Figure 2.

Modification of carbon–clay composite membrane

Nitration. The unmodified carbon–clay composite membrane was prepared using the procedure of Kishore et al.[15] and is nitrated (a mixture of NO and NO_2) using NO_x at 200°C and 1 atm pressure.[34,35] The carbon–clay composite membrane is placed inside the nitration reactor and the NO_x (~500 mL) is introduced through the silicon septum of the reactor by syringe and is kept in the oven at 200°C for 6 h. The formation of the nitrated carbon membrane is represented by reaction 1 of

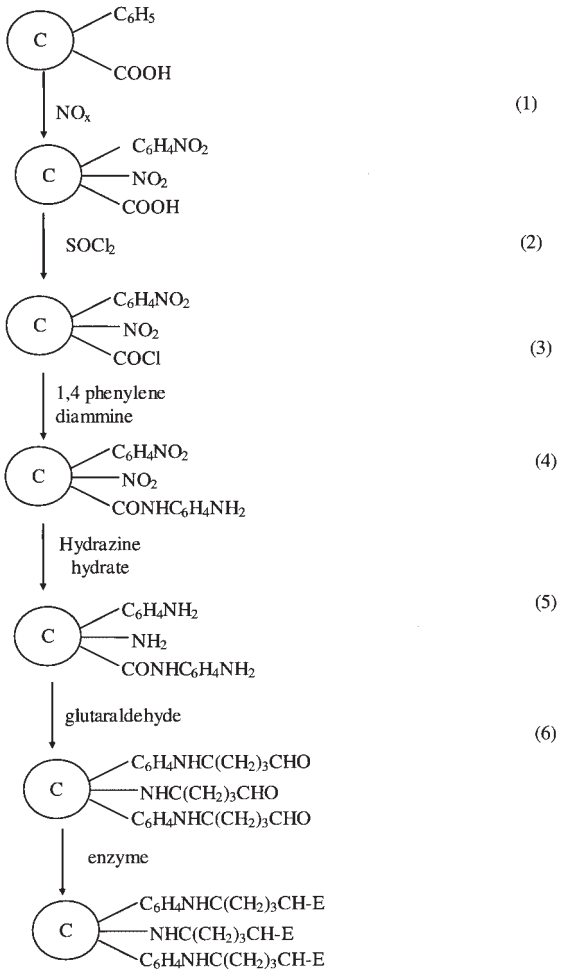

Figure 2. Immobilization of enzyme on the membrane surface.

E stands for enzyme and © for carbon membrane.

Figure 2. FTIR spectra of the modified carbon membrane were obtained using a Vector 22 spectrophotometer (Bruker, Rheinstetten, Germany) to confirm the covalent bonding of the NO_2 functional groups as shown in Figure 3b. The Raman spectra (Figure 4b) were also obtained by an Ar^+ laser beam at λ_{ex} = 514.5 nm (Perx 1877 triple mass spectrometer).

Neutralization. To remove the acid functional groups, the nitrated membrane thus formed is neutralized following the procedure given in Alves et al.[36] In this, it is reacted with thionyl chloride (10 cm^3, 0.14 mol) in toluene (80 cm^3) and refluxed at 100°C for 3.5 h. The acyl chloride group is formed as shown in reaction 2 of Figure 2. After this, it is rinsed with toluene (~100 cm^3), reacted with a solution of 1,4-phenylenediamine (210 mg, 1.9 mmol), dissolved in 100 mL of toluene, and refluxed at 100°C for 3.5 h. The reaction with this reagent occurs according to reaction 3 of Figure 2 and this way the acid is converted to its esters. Subsequently, it is removed, rinsed with toluene (~100 cm^3), and dried at room temperature for 16 h and then at 70°C for 24 h.

Amination. The nitrate groups produced by nitration are reduced with 50% hydrazine hydrate solution at 75°C for 4 h (see reaction 4 in Figure 2) to position the amine group onto the

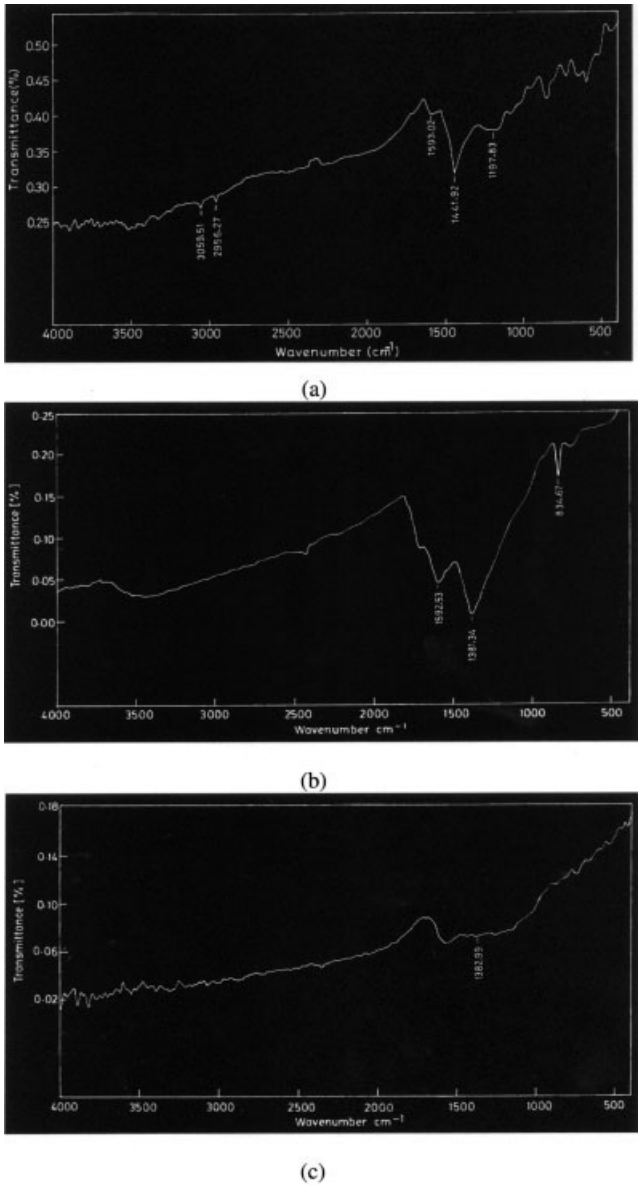

Figure 3. FTIR spectra of (a) unmodified (UM), (b) nitrated (NM), and (c) aminated (AM) carbon membrane.

membrane surface (called aminated membrane). To confirm the presence of these functional groups on the membrane, we carried out FTIR (Figure 3c) and Raman spectroscopy (Figure 4c).

Reaction with Glutaraldehyde. To position free aldehydes group on the membrane surface, the aminated membrane is reacted with glutaraldehyde reaction mixture (see reaction 5 of Figure 2). The reaction mixture (5% glutaraldehyde solution) was prepared by adding 20 mL of a 25% aqueous glutaraldehyde solution to 80 mL of a 0.05 M sodium phosphate buffer at pH 7. The aminated membrane is kept in the reaction mixture at room temperature for 3 h and stirred gently. After the reaction, the membrane is removed and washed thoroughly with 0.05 M sodium phosphate buffer to remove excess glutaraldehyde.

Enzyme loading and activity

Pancreatic lipase (supplied by S.D. Fine Chemicals) was used without further purification. The lipase solution is prepared by dissolving 5 g of lipase powder in 100 mL of 0.05 M sodium phosphate buffer at pH 7. The glutaraldehyde reacted membrane, kept in a beaker that contains 100 mL of lipase solution, is stirred gently for 8 h at 25°C. After the reactions

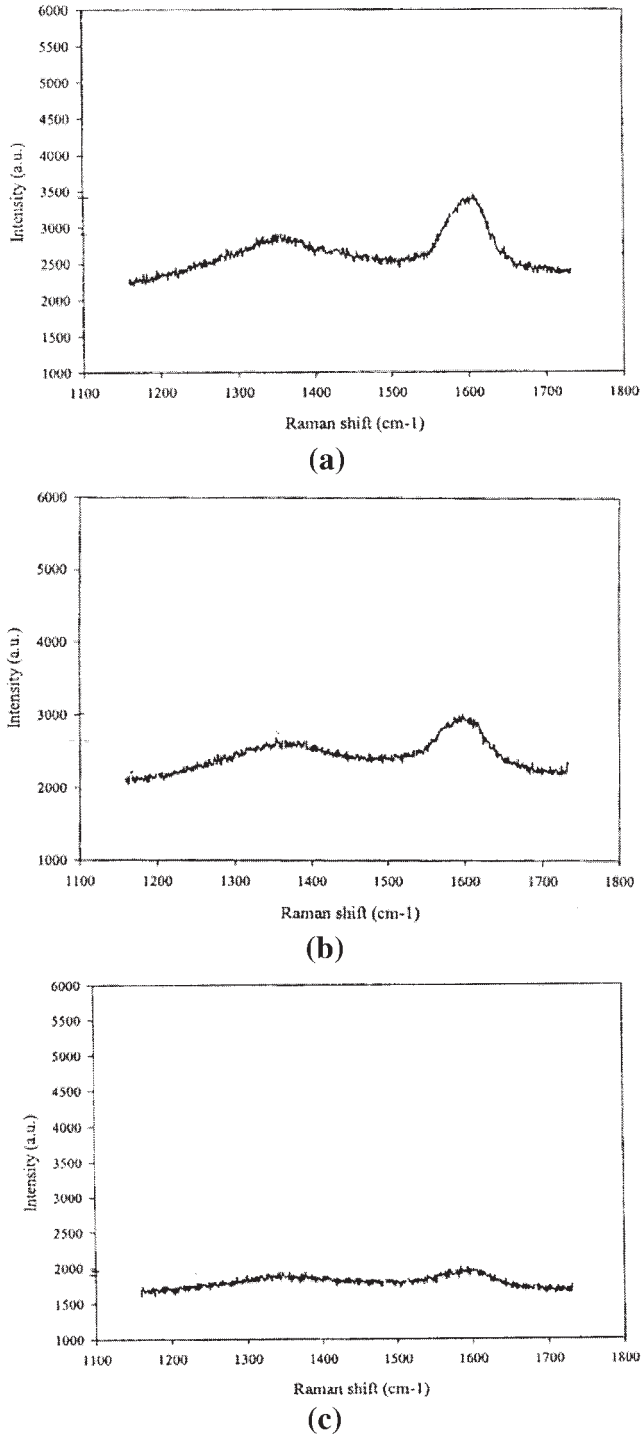

Figure 4. Raman spectra of (a) unmodified, (b) nitrated, and (c) aminated carbon membrane.

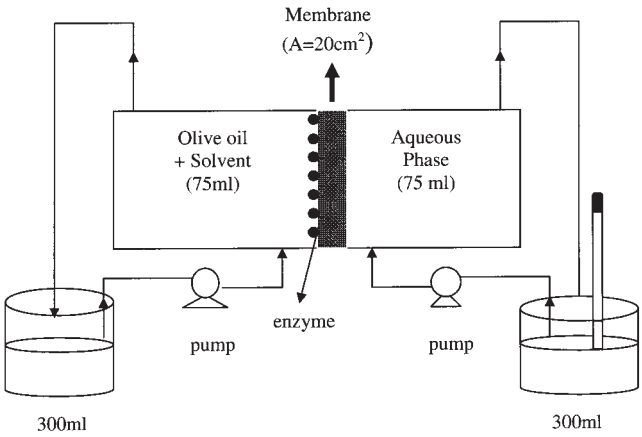

Figure 5. Biphasic membrane reactor.

(see reaction 6 of Figure 2), the membrane is removed and washed with a sodium phosphate buffer (pH = 7) solution.

Determination of Activity. The activity of enzyme is determined by standard tests, described in the Worthington Enzyme Manual,[37] that are based on reacting enzyme with an emulsion of olive oil in water stabilized by gum arabic and sodium chloride (3.0 M), calcium chloride (0.075 M), and sodium tauroglucate salt (0.027 M). The pH of the reaction mixture is adjusted to 8 and the volume of titrant (10 mM solution of NaOH) added is recorded for 3–4 min after a constant rate is achieved. The blank rate is determined as the volume of titrant added per minute from the final linear portion of the curve. The enzyme solution (5 mL) is added to the reaction mixture (15 mL), pH is adjusted to 8, and the volume of titrant required to maintain the pH 8 is recorded for 5–6 min. The sample rate is determined as the volume of titrant added per minute from the linear portion of the curve. The activity of the enzyme is calculated from the following equation:

$$\frac{\text{Units } (\mu\text{mol/min})}{\text{mg}} = \frac{[(\text{sample} - \text{blank}) \text{ rate (mL/min)}] \times \text{normality of base (mmol/L)} \times 1000}{\text{mg enzyme in reaction mixture}} \quad (5)$$

We first determined the activity of an enzyme solution. This solution was used to immobilize the enzyme on the membrane. The difference of the activity of the fresh solution and the supernatant solution would constitute the activity of the enzyme if it were in a free state. The activity of immobilized enzyme was also experimentally described using a similar procedure.[38]

Biphasic enzyme membrane reactor

The experimental setup (Figure 5) consists of two cylindrical compartments each having a capacity of 75 mL with the membrane (membrane area = 20 cm^2) held between these two compartments. The temperature of the reactor is maintained at a constant value of 30°C by using a water bath. In the compartment (maintained at 30°C) facing the active membrane surface, 300 mL of substrate (olive oil in organic solvents) is circulated at a rate of 400 mL/min, maintained constant throughout the experiments. In the other compartment, 300 mL of water at basic pH is circulated using a peristaltic pump. The pH of water is maintained at a constant value by adding 10 mM NaOH solution; the amount thus added is used to determine the amount of fatty acid extracted by water and the amount of free fatty acid produced per unit time.[9] The EMR performance is reported in terms of the amount of free fatty acid produced per unit time (mmol L^{-1} h^{-1}) based on the volume of the aqueous phase. The fatty acid production was calculated from

$$\text{Amount of fatty acid produced (mmol/L)} = \frac{\text{normality of NaOH (mmol/L)} \times \text{volume of NaOH added (mL)}}{\text{volume of aqueous phase (mL)}} \quad (6)$$

To study the influence of operating conditions, we varied various parameters pH of aqueous phase (8–9.5), solvent used for olive oil (pentane, hexane and heptane), substrate (olive oil) concentration (25–100%), and aqueous phase circulation rate (200–600 mL/min) around their base case values at a time. The base case values of the parameters have been taken as pH: 9; solvent: pentane; olive oil concentration: 50 vol %; aqueous phase circulation rate: 400 mL/min; temperature: 30°C. For the entire parameter studies the organic phase circulation rate is kept at 400 mL/min. To study the effect of all these parameters the reaction was carried out for 130 min at the base case conditions.

Results and Discussion

Preparation and modification of carbon membranes

We prepared carbon composite membranes as reported in Kishore et al.,[15] nitrated using NO_x, and aminated the carbon membrane as reported in earlier in the experimental section. The aminated membrane was reacted to glutaraldehyde and the lipase was chemically immobilized onto it. On experimentation, it was found that the enzyme became inactive after two cycles of operation. Based on the work reported in the literature[36] on activated carbon, the carbon membrane was expected to have phenyl and carboxylic groups on its surface (see reaction 1 of Figure 2). Expecting that the immobilized enzyme may have lost its activity as a result of low pH of the surface, we neutralized the carboxylic acid functional groups following the procedure given in Figure 2. In the case of unmodified carbon membrane (Figure 3a) an aliphatic C–H stretching is observed at 1441.92 cm^{-1}. Likewise, in the case of nitrated membrane, its FTIR spectrum (Figure 3b) clearly shows $–NO_2$ asymmetric configuration {weak $–C(NO_2)_3$} at 1592.53 cm^{-1} and $–NO_2$ symmetric stretching {strong $–CH_2–NO_2$} at 1381.84 cm^{-1}. A weak-medium type R–CHR–NO_2 stretching is observed at 834.67 cm^{-1}, thus confirming the presence of chemically bound nitro groups on the carbon membrane surface. Upon amination, no extra peaks for the amine group have been observed, although the nitro group peak disappeared. After aminating this membrane with 50% hydrazine hydrate solution, it is now possible to use this for immobilization of the enzyme. The enzyme immobilized onto it is found to be active even after 30 days of usage.

Raman spectroscopy is used to measure the degree of sp^2 to sp^3 binding in the membrane. Figure 4 shows the Raman spectra of the unmodified, nitrated, and aminated carbon mem-

branes. The normal spectrum of carbon usually consists of a strong peak in the range of 1580–1600 cm^{-1} and a weak peak in the range of 1350–1370 cm^{-1}. The former peak, called G-mode peak, which represents the graphite structure having sp^2 hybridization and the latter is the D-mode peak having sp^3 hybridization.[38] From Figure 4, we see the presence of the G-mode peak at 1591 cm^{-1} and the D-mode peak at 1367 cm^{-1}. Upon nitration, the peak intensity of both the D- and G-mode peaks is found to diminish, which is further reduced by the amination reactions. This reveals that the material is becoming more amorphous in nature by the chemical modification. The C–NO_2 bond appears at 1591 cm^{-1} for the nitrated carbon[39] and its height is considerably decreased for the aminated membranes attributed to C–NH_2 formation.

Immobilization of lipase

Lipase is covalently immobilized on the modified carbon membrane using glutaraldehyde as the bridging molecule between the enzyme and the membrane. The activity of the enzyme is determined by following the procedure described earlier and the rate of hydrolysis of an olive oil emulsion is determined by potentiometric titration. One unit releases one micromole of fatty acid per minute from olive oil at 25°C and pH 8.0 under the specified conditions. The activity of the fresh enzyme and the remaining solution after immobilization is found to be 12.27 and 10.01 U, respectively. The difference between these values gives the units of enzyme immobilized on the membrane and is determined to be 2.25 U. In a similar way, the activity of enzyme immobilized on the membrane was also determined, which was found to have increased to 3.20 U. It is seen that upon immobilization of enzyme on the modified carbon membrane, the activity increases 1.42-fold.

Effects of operating variables on the performance of the biphasic enzyme membrane reactor

The performance of the biphasic membrane has been evaluated in terms of the (mmol L−1 h−1) based on the volume of the aqueous phase used for the extraction of the fatty acid. A blank run is performed in which a membrane without enzyme is used and it was found that the pH of the aqueous phase does not change. When the membrane with the immobilized enzyme is used, the production of fatty acids shows a linear trend (see Figure 6) and is regressed using a linear function (with correlation coefficient ≅ 99%) to find the rate. The hydrolysis of triglycerides is a multistep reaction system with the formation of diglycerides (D) and monoglycerides (M) reversibly as intermediate steps. For short times, the concentration of the products (that is, fatty acid denoted by F) is small and the Michaelis–Menten kinetics can be used to describe the overall reaction rate as

$$v_0 = \frac{V_{\max}[S_0]}{K_M + [S_0]} \tag{7}$$

where v_0 is the initial rate of formation of products, $V_{\max}$ is the limiting initial velocity when the enzyme is fully saturated with the substrate, K_M represents a constant, and $[S_0]$ is the initial substrate concentration at the interface.

Influence of pH. In the case of the enzyme membrane reactor the NaOH and olive oil come in close contact at the interface where the reaction occurs because of the enzyme present at that site. The linear trend in Figure 6 appears to confirm this and the overall reaction mechanism. From the slopes of lines in Figure 6a, V_R as a function of pH has been plotted in Figure 6b. It can be seen from this figure that the amount of free fatty acid produced per unit time increases with increasing pH. The highly nucleophilic OH^- ions have been reported to attack fatty acid (RCOOH) to form $RCOO^-$ ions that are resonance stabilized.[26] Thus an increase in OH^- concentration would increase the rate of formation of $RCOO^-$ and will thus increase the driving force for the diffusion of fatty acid from the reaction site to the bulk of the aqueous phase.

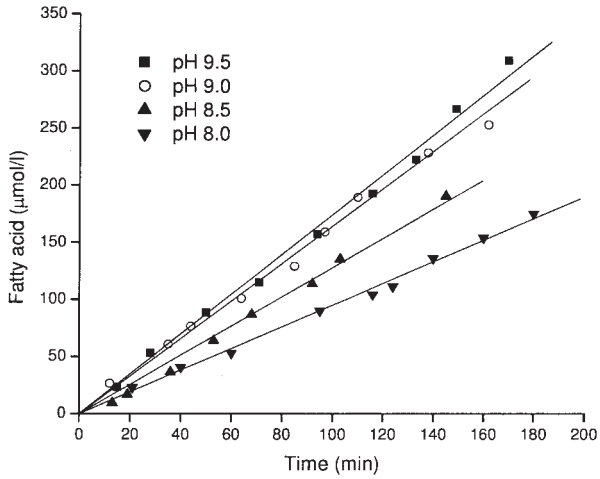

(a)

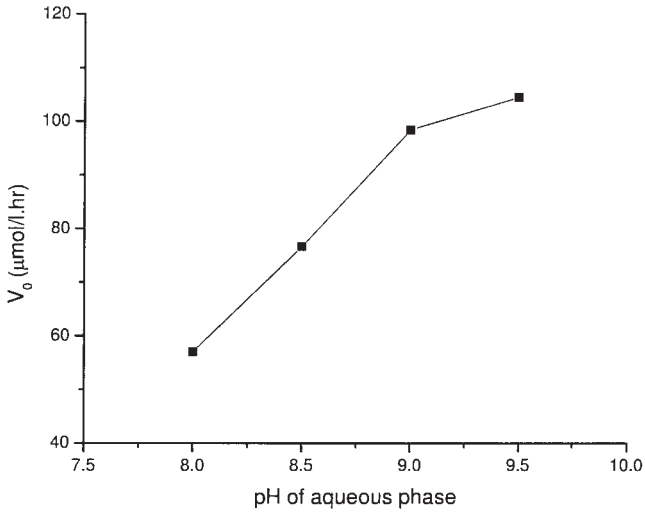

(b)

Figure 6. Effect of aqueous phase pH on the amount of free fatty acid produced per unit time (V_0) in biphasic EMR.

(a) Fatty acid concentration vs. time and (b) volumetric reaction rate (V_0) vs. pH.

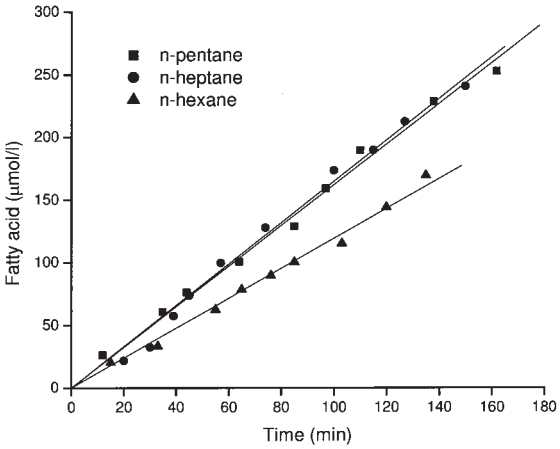

Figure 7. Effect of organic solvent (used for olive oil) on the amount of free fatty acid produced per unit time in biphasic EMR.

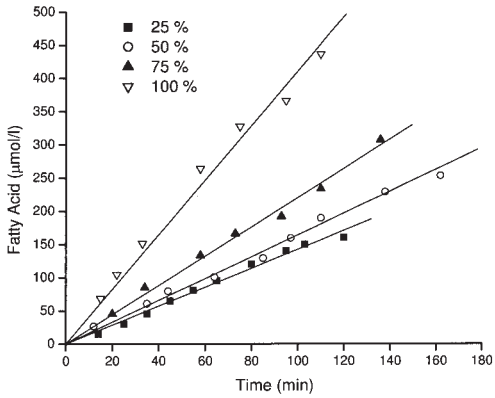

Figure 8. Effect of olive oil concentration on amount of free fatty acid produced per unit time in the biphasic EMR.

The base case rate is 50 vol % olive oil in *n*-pentane and circulation rate of both aqueous and organic phases is 400 mL/min at 30°C.

However, as pH is increased >9, the increase in V_R appears to slow down.

Influence of Solvent. It is known from the literature[40] that the organic solvents used as a medium of reaction with olive oil substantially affect the enzyme activity. To analyze the effect of solvent, three homologous nonpolar solvents (*n*-pentane, *n*-hexane, and *n*-heptane) are used that are known to dissolve the oil. The fatty acid production with time in a biphasic EMR using lipase-immobilized membrane is shown in Figure 7, where the plot is linearly regressed ($R > 0.99$) to determine the V_R. The amount of free fatty acid produced per unit time is found to depend heavily on the solvents used and it is higher for *n*-pentane and *n*-heptane than for *n*-hexane, for which the value is much lower. Thus, there exists no trend for the variation of V_R with the carbon number of the solvent. It is well understood that the active sites of the enzyme consist of a set of nonsequential amino acid [(serine, histadiene, aspartic acid) or (serine, histadiene, and glutamic acid)] residues[19] that promote hydrolysis. The shape of the enzyme molecule determines the concentration of these on the surface and the former depends heavily on the medium of reaction. These experiments suggest that in the medium of the pentane, the membrane catalyst works the best.

Influence of Olive Oil Concentration. To have an insight into the effect of concentration of olive oil, four different concentrations of olive oil (25, 50, 75, and 100 vol %) in the organic phase with pentane as solvent was used. The circulation rate of both phases is kept at 400 mL/min and the temperature is maintained at 30°C. Figure 8 shows the fatty acid production with time in the biphasic EMR. The reaction rate of olive oil hydrolysis increases with substrate concentration in the range of concentration tested (25 to 100 vol %) because a higher substrate concentration improves the reaction rate. After 50 vol % of substrate concentration, the increase in reaction rate is high. The maximum reaction rate was 0.246 mmol L^{-1} h^{-1}, which was obtained at 100 vol % substrate concentration.

If we assume the entire olive oil concentration up to the interface the average concentration ($=[S_0]_{\text{interface}}$) and the reaction to be described by Eq. 7, then one has the following:

$$\frac{1}{v_{0,\text{interface}}} = \frac{1}{V_{\max}} + \frac{K_M}{V_{\max}} \frac{1}{[S_0]_{\text{interface}}} \tag{8}$$

Because we have a steady state in the system, the v_0 at the interface, $v_{0,\text{interface}}$, is the same as that determined in our experiment and this equation can be used to evaluate K_M and $V_{\max}$ on plotting $1/v_0$ vs. $1/[S_0]$. We have thus determined the value of K_M as 3.74 mol/L and the value of $V_{\max}$ as 3.66 μmol L^{-1} min^{-1} using regression analysis with $R^2 = 0.654$.

Influence of Circulation Rate. Figure 9 shows the data for the fatty acid production with time for the three different circulation rates. For this study, the organic phase circulation rate is kept at 400 mL/ min. It is found that the reaction rate increases with increasing water circulation rate. A higher water circulation rate would decrease the boundary layer on the aqueous side of the membrane, causing a reduction in the mass transfer resistance and an increase in the mass transfer rate of the fatty acid.

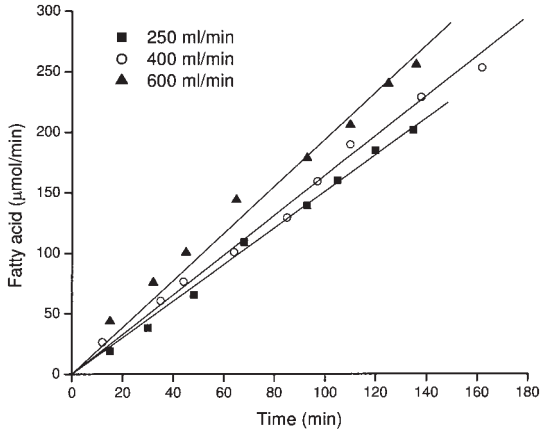

Figure 9. Effect of aqueous phase circulation rate on the amount of free fatty acid produced per unit time in the biphasic EMR.

The organic phase circulation rate is kept at 400 mL/min.

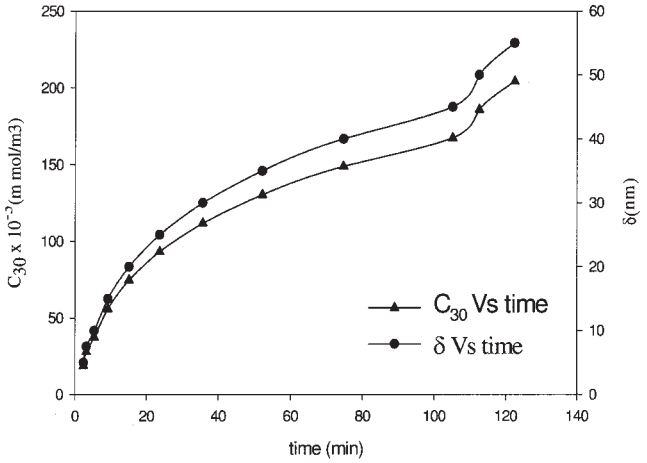

Figure 10. Growth of film in region I and variation of concentration of ion 3 at the boundary of region I of the aqueous phase.

Determination of mass transfer rate and wall potential

The flux of ion 2 (OH^-) can be calculated from the rate of addition of NaOH because the pH of the aqueous phase is constant. The experimental data show that for all cases, the rate of addition of NaOH is constant and thus the flux of ion 2 is constant and for the base case it is calculated to be 1.365×10^{-11} kmol m^{-2} s^{-1}. It is found that the penetration of ion 3 into the aqueous phase is less than the film thickness values determined from the mass transfer coefficient given in the literature,[32] valid for a cross-flow membrane system (Eqs. 6 and 7). The film thickness (equal to the depth of penetration of ion 3) is therefore determined by the solution scheme previously given in detail in our earlier publication.[13] The various physical and experimental data required for calculation are diffusion coefficient of ions (D_1 = 1.332e-9, D_2 = 5.2964e-9, D_3 = 1.79e-11 m^2/s), rate of addition of NaOH ($\beta = 2.6997 \times 10^{-8}$ kmol m^{-3} s^{-1}), area of aqueous compartment (A_c = 20 cm^2), volume of aqueous compartment (V_{aq} = 300 mL), universal gas constant ($\Re$ = 8314), and temperature (T = 303 K). The diffusion coefficients of ions 1 and 2 are evaluated from infinite dilution equivalent conductance values given in the

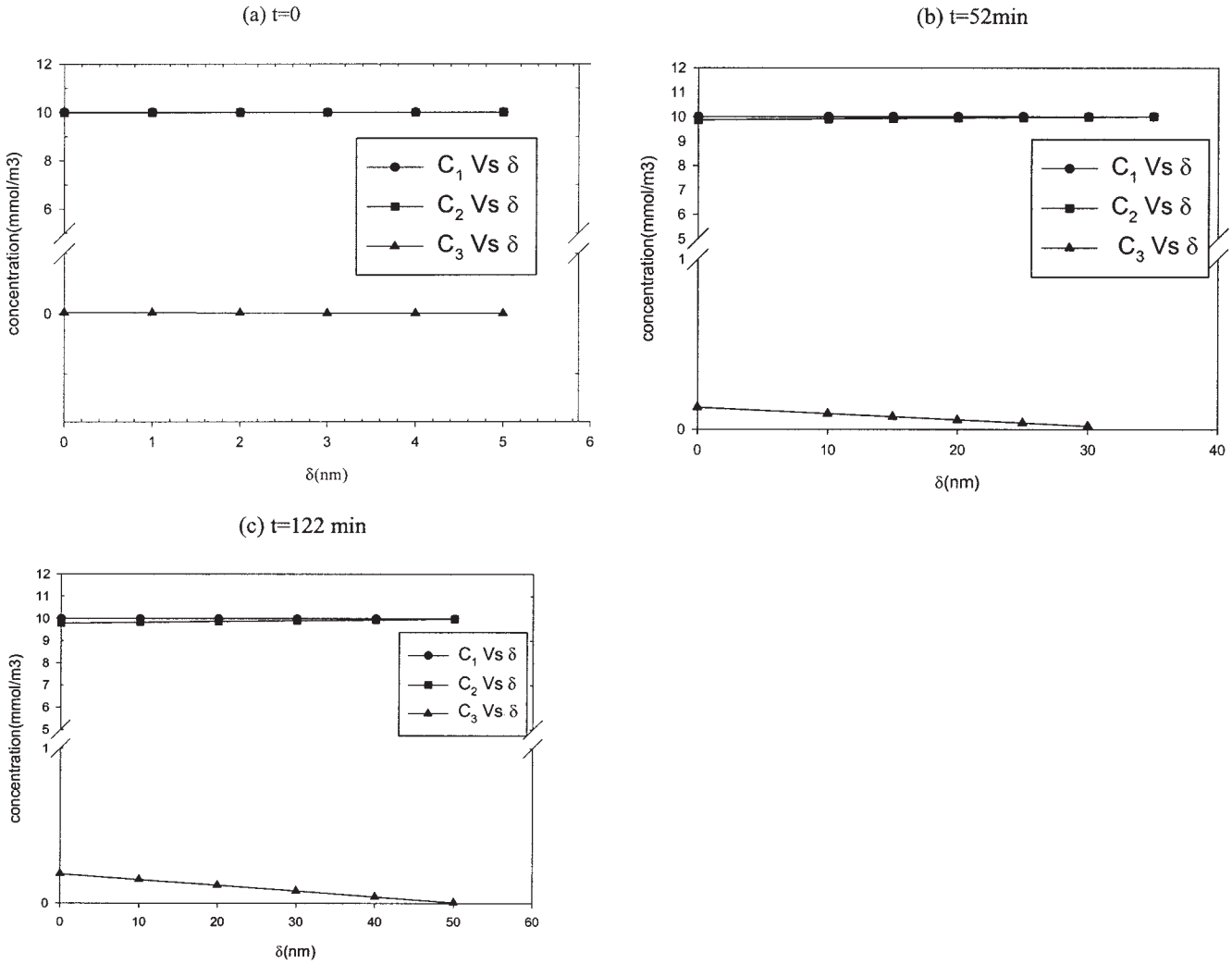

Figure 11. Concentration profiles of the ions in region I at three different times: t = 0, t = 52 min, and t = 122 min.

The profiles were determined using the base case experimental data.

literature and that of ion 3 is assumed to be equal to the diffusion coefficient of oleic acid.

Figure 10 shows the growth of film thickness with time for the base case. The time zero is taken as the instant when the ion 3 concentration at $x = 0$ is (0.01 mmol/m^3) such that the film thickness is more than 10-fold the approximate ion size ($\sim$0.6 nm). The film thickness after 2 h is about 70 nm and is considerably smaller than the value obtained from the mass transfer correlation ($\sim$2.05 μm). Figure 10 also shows the variation of ion 3 concentration at $x = 0$ with time and it may be seen from the figure that it follows a trend similar to that of film thickness. It increases rapidly at the beginning and then levels off with time.

Figure 11 shows the concentration profile of the three ions at three different times. It may be seen that the ion concentration varies in such a way that the sum of concentrations of ions 2 and 3 is equal to the concentration of ion 1. It may also be noticed that, although initially, the ion 1 and 2 concentrations are almost the same, as the time increases the difference between the two increases as the result of an increase in the concentration of ion 3. The value of electric field calculated from the simulation is about 8×10^3 V/m. This corresponds to a value of $(C_1 - C_2 - C_3)$ (deviation from electro-neutrality) of nearly 10^{-14} kmol/m^3, which is $<$0.001% of the average ion concentration prevailing inside the film. Thus, the film (region I) may be assumed to be electro-neutral.

It may also be noticed that the fluxes of these ions are extremely small compared to their concentrations in the film ($\sim 10^{-6}$ kmol m^{-2} s^{-1}) and so the pseudo-steady-state assumption at the boundary of regions II and I can be made. For the determination of wall potential and mass-transfer rate in region II, the pore radius of the membrane is taken as equal to the average of the pore size range (4 nm) of the membrane that is determined in a previous work.[15] The pore length is determined from the cross-sectional view of the membrane and is found to be 40 μm, whereas the porosity of the membrane is determined to be 0.4. The wall potential, determined this way, is found to be 0.71 mV for the various sets of experimental data of this work. This was calculated using the solution scheme already described in an earlier work.[13]The space charge model uses the potential of the double layer in the aqueous phase and the low value of the wall potential is therefore attributed to the extremely low concentration of the ions in the aqueous phase. The wall potential value is found not to change significantly within 20% change in pore radius.

Conclusion

A noninterpenetrating supported modified carbon membrane is prepared for the immobilization of lipase using glutaraldehyde as the bridging molecule between the enzyme and the membrane. The membrane was modified so as to neutralize the acid functional groups using 1,4-phenylenediamine, which ensured a better immobilization and longer life of the enzyme. Experiments show that the activity of lipase increases 1.42-fold upon immobilization. Hydrolysis of olive oil was carried out in a biphasic enzyme membrane reactor and its performance was evaluated in terms of the amount of free fatty acid produced per unit time based on the volume of aqueous phase used for extraction of fatty acids. The effect of various operating parameters (pH, solvent, olive oil concentration, and circulation rate of aqueous phase) was evaluated. The maximum reaction rate was 3.6-fold higher, and the base case rate was 1.4-fold higher than the values reported in the literature for a similar enzyme membrane reactor but a different membrane. The immobilized enzyme was found to be highly stable for a period of 30 days without much change in the activity of the enzyme. A model is proposed to describe the mass transfer of ions on the aqueous side of the reaction sites. Film theory was used to describe the transport of ions in the first region and a space charge model for the second region; the wall potential determined from the model was 0.71 mV.

Literature Cited

1. Prazeres DMF, Cabral JMS. Enzymatic membrane bioreactors and their application. *Enzyme Microb Technol.* 1994;16:738.
2. Giomo L, Drioli E. Biocatalytic membrane reactors: Applications and perspectives. *TIBTECH.* 2000;18:339-349.
3. Baily JE, Ollis DF. *Biochemical Engineering Fundamentals*. 2nd Edition. New York, NY: McGraw-Hill; 1986.
4. Villeneuve P, Muderhwa JM, Graille J, Haas MJ. Customising lipase for biocatalysis: A survey of chemical, physical and molecular biological approaches. *J Mol Catal B: Enzymatic* 2000;9:113-148.
5. Hoq MM, Koike M, Yamme T, Shimizu S. Continuous hydrolysis of olive oil by lipase in microporous hydrophobic hollow fiber bioreactor. *Agric Biol Chem.* 1995;49:3171-3178.
6. Rucka M, Turkiewicz B. Ultrafiltration membranes as carriers for lipase immobilization. *Enzyme Microb Technol.* 1990;12:52-55.
7. Tsai S, Shaw SS. Selection of hydrophobic membranes in the lipase catalyzed hydrolysis of olive oil. *J Membr Sci.* 1998;146:1-8.
8. Mercon F, Erbes VL, Sant, Anna GL Jr, Noberega R. Lipase immobilized membrane reactor applied to babassu oil hydrolysis. *Braz J Chem Eng.* 1997;14:1-11.
9. Pronk W, Kerkhof PIAM, Vanhelden C, Van't Riet K. The hydrolysis of triglycerides by immobilized lipase in a hydrophilic membrane reactor. *Biotechnol Bioeng.* 1988;32:512-518.
10. Giorno L, Molinari R, Natoli M, Drioli E. Hydolysis and regioselective transestrification catalyzed by immobilized lipase in membrane bioreactor. *J Membr Sci.* 1997;125:177-187.
11. Guit RPM, Kloosterman M, Meindersma GW, Mayer M, Meijer EM. Lipase kinetics: Hydrolysis of triacetin by lipase from candida cylindracea in a hollow-fiber membrane reactor. *Bioengineering.* 1991;38: 727-732.
12. Bouwer ST, Cuperus FP, Derksen JTP. The performance of enzyme-membrane reactors with immobilized lipase. *Enzyme Microb Technol.* 1997;21:291-296.
13. Shukla A, Kumar A. Experimental studies and mass transfer analysis of the hydrolysis of olive oil in a biphasic zeolite membrane reactor using chemically immobilized lipase. *Ind Eng Chem Res.* 2004;43: 2017-2029.
14. Pugazhenthi G, Kumar A. Enzyme membrane reactor for hydrolysis of olive oil using lipase immobilized on modified PMMA composite membrane. *J Membr Sci.* 2004;228:187-197.
15. Kishore N, Sachan S, Rai KN, Kumar A. Synthesis and characterization of a nanofiltration carbon membrane derived from phenol-formaldehyde resin. *Carbon.* 2003;41:2961-2972.
16. Salmon PR, Robertson CR. A theoretical analysis of a hollow fiber membrane reactor with two substrates. *Chem Eng J.* 1987;35:B1-B8.
17. Salzman G, Tadmor R, Guzy S, Sideman S, Lotan N. Hollow fiber enzymic reactors for two substrate processes: Analytical modeling and numerical simulations. *Chem Eng Process.* 1999;38:289-299.
18. Malcata FX, Hill CG, Amundson CH. Use of a lipase immobilized membrane in a membrane reactor to hydrolyze the glycerides of butteroil. *Biotechnol Bioeng.* 1991;38:853-868.
19. Malcata FX, Reyes HR, Garcia HS, Hill CG, Amundson CH. Kinetics and mechanism reactions catalyzed by immobilized lipases. *Enzyme Microb Technol.* 1992;14:426-446.
20. Paiva AL, Balcao VM, Malcata FX. Kinetics and mechanism of reactions catalyzed by immobilized lipases: Review. *Enzyme Microb Technol.* 2000;27:187-204.
21. Ceynowa J, Adamczak P, Staniszewski M. Kinetics of olive oil hy-

drolysis in an enzyme membrane reactor bond graph network model of reactor performance (Part I). *Acta Biotechnol.* 1997;17:161-176.
22. Ceynowa J, Adamczak P. Analysis of the bond graph network model of the membrane reactor for olive oil hydrolysis. *Sep Purif Technol.* 2001;22/23:443-449.
23. Fomuso LB, Akoh CC. Lipase-catalyzed acidolysis of olive oil and caprylic acid in a bench-scale packed bed bioreactor. *Food Res Int.* 2002;35:15-21.
24. Jensen BH, Galluzzo DR, Jensen RG. Studies on free and immobilized lipase from Mucor miehei. *J Am Oil Chem Soc.* 1988;65:905-910.
25. Yamane T, Hoq MM, Shimizu S. Kinetics of continuous hydrolysis of olive oil by lipase in microporous hydrophobic membrane bioreactor. *Yukagaku.* 1986;35:10-17.
26. Molinari R, Santoro ME, Drioli E. Study and comparison of two enzyme membrane reactors for fatty acid and glycerol production. *Ind Eng Chem Res.* 1994;33:2591-2599.
27. Morrison RT, Boyd RN. *Chimica Organica*. 5th Edition. Milan, Italy: Editrice Ambrosiana; 1991.
28. Klibanov EM. Enzyme catalysis in anhydrous organic solvents. *Trends Biochem Sci.* 1989;14:141-147.
29. Tsai SW, Chang CS. Kinetics of lipase-catalyzed hydrolysis of lipids in biphasic organic-aqueous systems. *J Chem Tech Biotechnol.* 1993; 57:147-154.
30. Hsu T, Tsao GT. Convenient method for studying enzyme kinetics. *Biotechnol Bioeng*. 1979;21:2235-2246.
31. Reid RC, Prausnitz JM, Poling BE. *The Properties of Gases and Liquids*. 4th Edition. New York, NY: McGraw-Hill; 1987.
32. Porter MC. Membrane filtration. In: Schweitzer PA, ed. *Handbook of Separation Techniques for Chemical Engineers*. 2nd Edition. New York, NY: McGraw-Hill; 1988:2-41.
33. Knop A, Pilato LA. *Phenolic Resins*. New York, NY: Springer-Verlag; 1985.
34. Chowdhury SR, Kumar P, Bhattacharya PK, Kumar A. Separation characteristics of modified polysulfone ultrafiltration membrane using NO_X. *Sep Purif Technol.* 2001;24:271-282.
35. Sinha S, Kumar A. Preparation of high capacity chloromethylated strong base anion exchange resin using NO_X. *Sep Sci Technol.* 2002; 37:895-919.
36. Alves JAC, Freire C, de Castro B, Figueiredo JL. Anchoring of organic molecules on activated carbon. *Colloids Surf A: Physiochem Eng Aspects* 2001;189:75-84.
37. Von Worthington CC, ed. *Worthington Enzyme Manual: Enzymes and Related Biochemicals*. Freehold, NJ: Worthington Biochemical Corp.; 1993. http://www.worthington-biochem.com/manual/L/PL.html
38. Ma C-CM, Lin J-M, Chang W-C, Ko T-H. Carbon/carbon nanocomposites derived from phenolic resin-silica hybrid ceramers: Microstructure, physical and morphological properties. *Carbon*. 2002;40: 977-984.
39. Baraksha H, Labudzinska A, Terpinski J. *Laser Raman Spectrometry Analytical Applications*. Warsaw, Poland: PWN-Polish Scientific Publishers; 1987.
40. Carrea G, Riva S. Properties and synthetic application of enzymes in organic solvents. *Angew Chem Int Ed Engl*. 2000;39:2226-2254.

Manuscript received Feb. 7, 2005, and revision received Oct. 19, 2005.